Chemical Physics Letters 603 (2014) 57–61

Contents lists available at ScienceDirect

Chemical Physics Letters

journal homepage: www.elsevier.com/locate/cplett

Polarity and oxidation level of visible absorbers in model organic aerosol

F. Rifkha Kameel [a], S.H. Lee [b], M.R. Hoffmann [a], A.J. Colussi [a,*]

[a] Linde Center for Global Environmental Science, California Institute of Technology, Pasadena, CA 91125, USA
[b] College of Public Health, Kent State University, 302/304 Williams Hall, Kent, OH 44242, USA

ARTICLE INFO

Article history:
Received 11 February 2014
In final form 18 April 2014
Available online 24 April 2014

ABSTRACT

How to parametrize the absorptivity of organic aerosols in atmospheric radiative models remains uncertain. Here we report that the $\lambda = 400$ nm absorbers in model aerosol mixtures elute as weakly polar species in reversed-phase chromatography. Typical among them, the $m/z = 269$ ($C_{12}H_{13}O_7^-$, O/C = 0.58) isomers detected by mass spectrometry possess C=O groups linked by C=C bridges. More polar species, such as the $m/z = 289$ ($C_{11}H_{13}O_9^-$, O/C = 0.82) polyacids, are instead colorless. On this basis we argue that visible absorptivity, which develops from extended conjugation among chromophores, may not increase monotonically with oxidation level.

1. Introduction

In addition to degrading air quality [1], aerosols affect the Earth's radiation budget [2,3]. They scatter incoming solar radiation, thereby having a cooling effect. Some [4,5], however, also absorb radiation and may have a significant warming effect on mid-troposphere [6]. Absorptivity is mainly due to their organic matter content. The main absorber is primary Black Carbon (BC) emitted during the incomplete burning of biomass materials. Aerosols, however, also contain Brown Carbon (BrC) matter [7] generated in the atmospheric processing of the volatile organic compound (VOC) emissions that dominate the tropospheric carbon budget [8].

The photochemical oxidation of VOC's should produce BrC aerosol particles whose optical properties may not be generic, but could vary with their residence time and the oxidative power of the local troposphere. Thus, there is a need for assessing how the evolution of BrC absorptivity could be parametrized in current atmospheric radiative transfer models. Extreme chemical complexity precludes a bottom up approach in which absorptivity is evaluated from the contributions made by the myriad light absorbers [9,10]. An alternative, more realistic approach is based on overall descriptors, such as overall polarity or oxidation level. Here we show that visible absorptivity may be associated with the less polar fraction of BrC components rather than with specific compounds. We also argue on chemical grounds that such fraction consists of highly unsaturated rather than highly oxidized species, and that the degree of unsaturation may be actually anti-correlated with oxidation beyond a certain level.

How chromophores absorbing in the visible ($\lambda > 400$ nm) are produced in the photochemical oxidation of VOCs is not fully understood [11,12]. It has been suggested that absorbance could involve unspecified interactions in the aerosol phase among discrete, low-molecular weight α-keto carboxylic acids [11], such as the widespread pyruvic and mesoxalic acids byproducts of the oxidation of aromatics [8,13,14]. These acids absorb (λ_{max} ~320 nm) the solar radiation reaching the lower troposphere due to the fact that the carbonyl chromophore is conjugated with the adjacent carboxyl C=O group, and thereby may undergo photochemistry [15]. Aqueous solutions of such acids and their photochemical transformations may in fact be considered model surrogates of typical aerosol matter. The photolysis of pyruvic acid solutions is known to produce small polyfunctional oligomers [16–20]. Previously, we had shown that visible absorptions develop during the thermal aging of such mixtures via the slow dehydration of alcohol functionalities [16,17]. We hypothesized that such red-shifted absorptions arose from the conjugation of disjoint carbonyl chromophores via newly created π-orbital >C=C< bridges in species, which, by being the products of dehydration, had lower O/C ratios than their precursors. Here, we confirm such hypothesis by means of separative analyses of aged model aerosol mixtures via high-performance reversed-phase liquid chromatography with tandem UV–visible absorption–electrospray/chemical ionization mass spectrometric detection.

2. Experimental details

Pyruvic acid (PA) solutions (0.1–0.5 M, PA, 98% Sigma–Aldrich) were prepared in deionized water adjusted to pH 1 using 70% $HClO_4$, sparged with ultrapure air prior and subsequently photolyzed with $\lambda > 305$ nm light. Sample solutions (3.5 mL,

* Corresponding author.
E-mail address: ajcoluss@caltech.edu (A.J. Colussi).

http://dx.doi.org/10.1016/j.cplett.2014.04.033
0009-2614/

magnetically stirred in 4 mL silica UV cuvettes kept at 298 K in a Peltier sample holder) (hereafter designated as P0) were irradiated for ~4 h with light from a 1 kW high-pressure Xe–Hg lamp source filtered through a water cell (to remove infrared radiation) and a tandem $\lambda > 305$ nm long band-pass interference filter. After irradiation, photolyzed samples (P1) were aged in the dark at 60 °C for several hours (16–19 h). Some of these thermally aged samples (hereafter P1-T1) were photolyzed for 1 h into P1-T1-P2 samples. Some P1-T1-P2 samples were thermally aged for several hours (P1-T1-P2-T2). Some P1-T1 samples were diluted in 1:5, 1:25 and 1:100 with deionized water prior to analysis.

Samples were analyzed by injecting 50 µl into a HPLC/UV/ESI (Agilent 1100 series) LC/MS system. Separation was performed using a ZORBAX Eclipse XDB-C18 RPLC reversed-phase column (l = 250 mm, ID = 3.00, dp = 5 micron, flow rate = 0.4 l/min, t_0 = 2.5 min) under various solvent gradient protocols. The eluent consisted of mixtures of solution A (0.1% acetic acid/ Milli-Q water) plus MeOH (B) programmed as follows: 7.5% B until 8 min, increasing to 90% at 45 min. ESI-MS detection of both positive and negative singled-charged ions in the 100–800 Da range was performed at various fragmentation voltages. We also run extracted ion chromatograms (EIC) at several m/z values. The structures of selected products were elucidated via MS/MS spectrometry using an Ion Trap detector (Agilent 6300 Series HPLC-MS^n/Bruker Ion Trap mass spectrometer) ran in positive and negative ion modes in the 30–800 Da mas range at fragmentation voltages of 1 and 3 V.

3. Results and discussion

We verified that PA solutions before (P0) or after being photolyzed (P1) do not absorb above λ ~350 nm, in accord with previous experiments from our laboratory performed under similar or identical conditions on PA samples as received from the supplier or distilled at low pressure [15,16]. The accelerated aging at 60 °C undergone by P1-T1 samples is deemed to simulate the thermal processes occurring in actual aerosol particles during their atmospheric lifetimes, which range from days to weeks depending on particle size and meteorology [21]. Previously, we had shown that the thermal 'browning' of such solution has an apparent activation energy E_{act} ~55 kJ mol^{-1} [17]. Thus, aging at 60 °C for 16 h is deemed equivalent to aging at 25 °C for ~5.6 days in the atmosphere.

In contrast with P0 and P1 samples, P1-T1 samples absorb appreciably up to ~450 nm. Figure 1 displays a chromatogram of P1-T1 solutions as simultaneously reported by absorbance at 400 nm (Figure 1A) and 254 nm (Figure 1B), and by the total negative ion current (TIC) detected by tandem ESI mass spectrometry (Figure 1C). It is apparent that (with the exception of a small feature at 6 min) *all* the species absorbing at 400 nm (1) elute after ~20 min, i.e., they are weakly polar [22,23], (2) are not well resolved under present conditions, i.e., they consist of a suite of molecular structures possessing a quasi-continuum of affinities for the column (3) they are acidic but, since they are weakly polar, the (carboxylic) acid groups appear to be attached to large, less polar backbones. Since $A_{254\ nm}/A_{400\ nm}$ ~10 for most chromophores (Figure 2), we overlaid the 10× chromatogram at 400 nm of Figure 1A in Figure 1B for comparison purposes. It is apparent that the lower red trace, which represents the estimated contribution of 400 nm absorbers to absorbance at 254 nm, implies that 400 nm absorbers amount to a minor fraction of the species present in this system. By the same token, we infer that nearly *all* the species that elute after 40 min absorb at 400 nm. Figure S1 shows the evolution of the 400 nm absorbers upon successive thermal aging and >300 nm photolysis treatments. As a rule, thermal aging results in the deepening of color, which is nearly bleached upon photolysis in accord with previous reports from our laboratory [17].

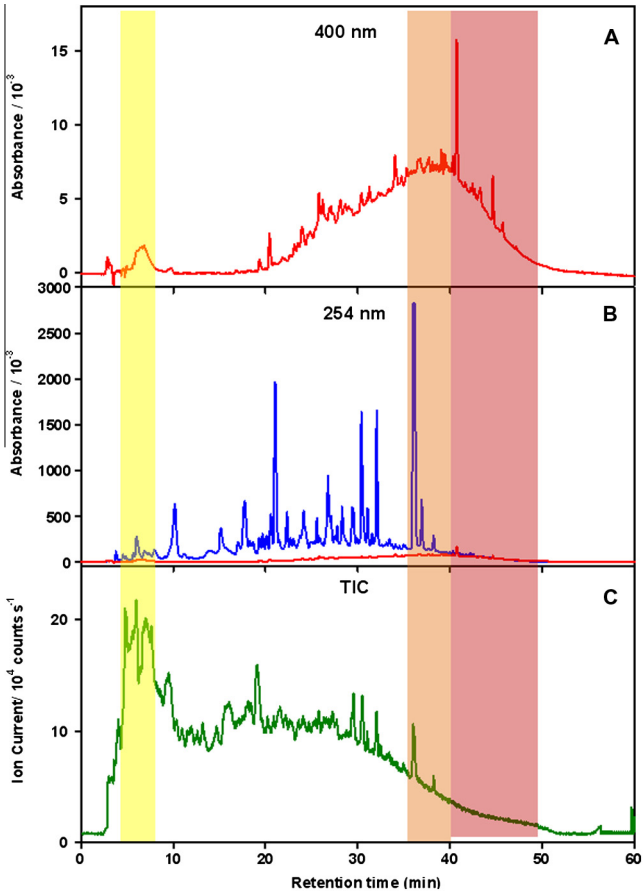

Figure 1. A typical chromatogram of a P1-T1 solution with product detection via UV absorption at 400, 254 nm and total (negative) ion current (TIC) ESI mass spectrometry. Colored bands denote retention time ranges. Yellow: 8–10 min, Orange: 35–40 min, Red: 40–50 min.

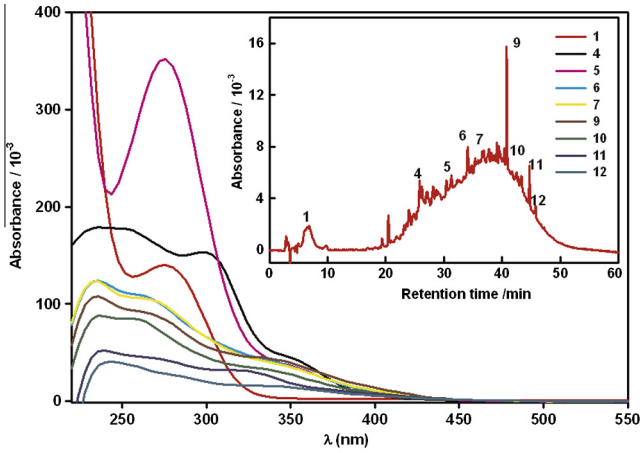

Figure 2. UV–Visible absorption spectra of species absorbing into the visible in P1-T1 mixtures (aged at 60 °C for 16 h).

Figure 3A–C show negative ion ESI mass spectra in the mass range m/z = 50 to 800 Da acquired between 8 and 10 min (yellow band in Figure 1) Figure 3A, between 35 and 40 min (orange band in Figure 1) Figure 3B, and between 40 and 50 min (red band in Figure 1) Figure 3C. Note the differences between the scales of the *Y*-axis of Figure 3A–C, which give a measure of the relative

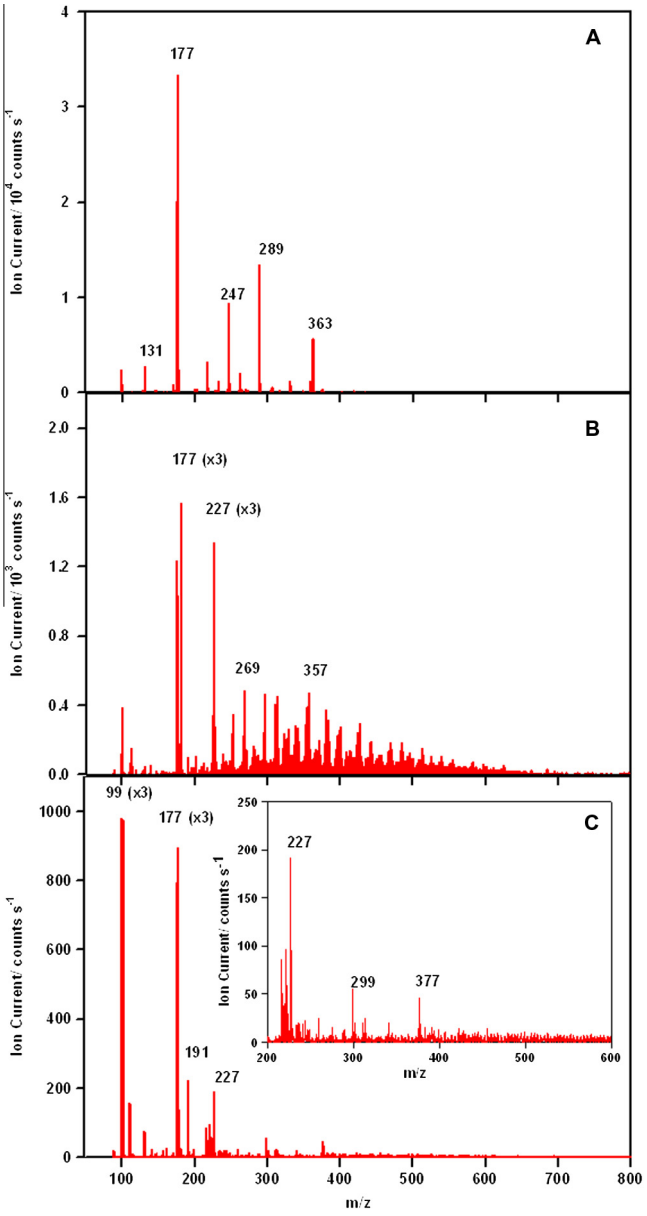

Figure 3. Negative ion chromatogram of species in P1-T1 mixtures (aged at 60 °C for 16 h). A: eluting within 4.5–8.5 min. B: 35–40 min; C: 40–50 min.

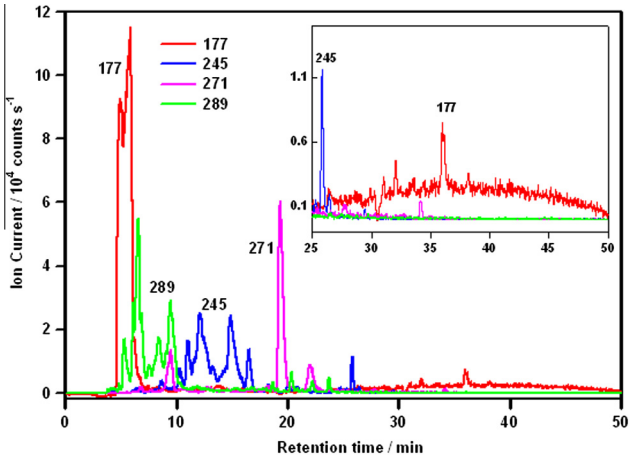

Figure 4A. Negative extracted ion chromatogram (EIC) of some of the most abundant polar species in P1-T1 mixtures (aged at 60 °C for 16 h). The insert zooms in the 25–50 min retention time range.

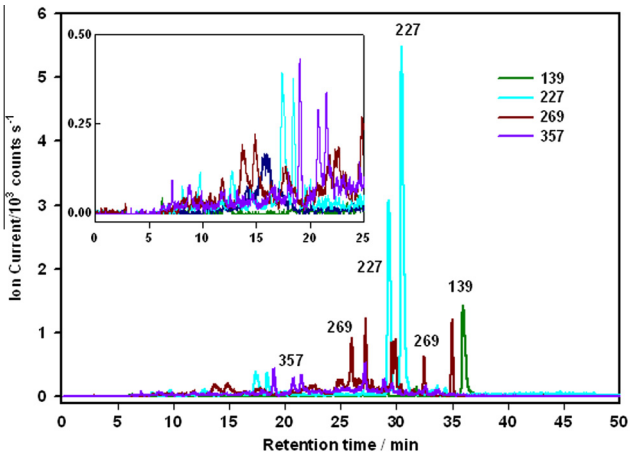

Figure 4B. Negative extracted ion chromatogram (EIC) of some of the most abundant weakly polar species in P1-T1 mixtures (aged at 60 °C for 16 h). The insert zooms in the 0–25 min retention time range.

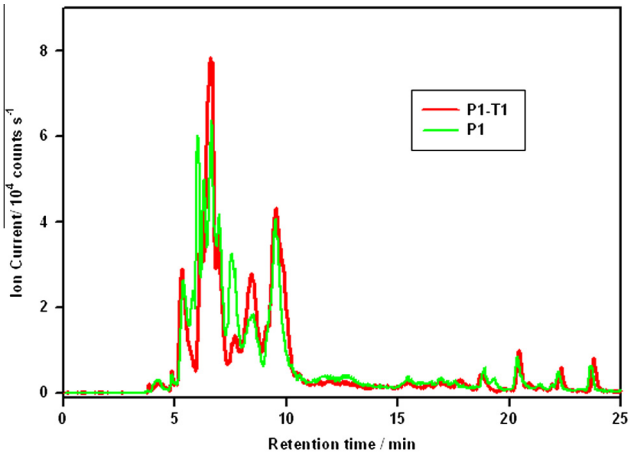

Figure 5A. Negative extracted $m/z = 289$ ion chromatogram (EIC) in P1 and P1-T1 solutions.

abundances of the anions detected in each case. If not the most intense, the most congested mass spectrum is that corresponding to those species eluting between 35 and 40 min (Figure 3B), which give rise to maximum absorbance at 400 nm (Figure 1A). EIC's are particularly informative about isomerism and polarity among the products (Figures 4A and 4B). Among the more polar species (i.e., those eluting before ~20 min) we find the isomers of $m/z = 289$ (green trace) and $m/z = 245$ (blue trace) anions (Figure 4A). Notably, $m/z = 177$ anions appear (mostly) at ~6 min, and also at ~36 min. It is hardly conceivable such $m/z = 177$ signals could correspond to a very polar and a weakly polar isomer of the same molecular formula, respectively (see below).

Figures 5A and 5B show the EIC's of the polar $m/z = 289$ and of the less polar $m/z = 269$ anions in P1 (after photolysis) versus P1-T1 (i.e., after thermal aging) samples, respectively. Note that the polar $m/z = 289$ anions of Figure 5A, which elute before 10 min, do not absorb appreciably at 400 nm (cf. Figure 1A), whereas some of the less polar $m/z = 269$ anions elute in the >20 min range which overlaps the region of significant 400 nm absorbance (Figure 1A). Also note that the intensities of

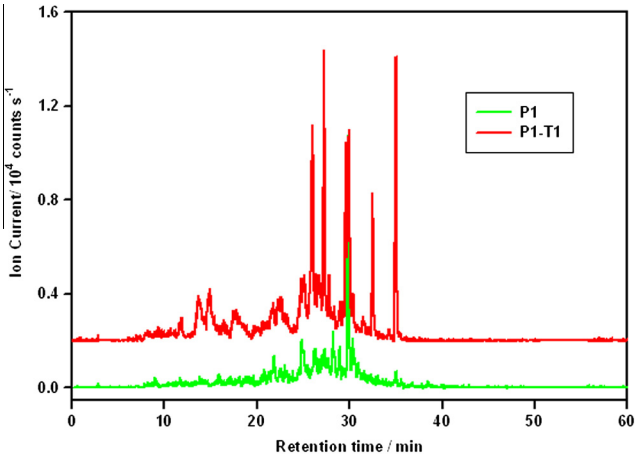

Figure 5B. Negative extracted $m/z = 269$ ion chromatogram (EIC) in P1 and P1-T1 solutions.

$m/z = 289$ anions do not change much upon aging, whereas those of the $m/z = 269$ anions markedly increase under the same conditions. Thus, the formation of $m/z = 269$ anions, as a representative of the species absorbing in the visible, is concomitant with color development during thermal aging. Hence, *the anions of mass 269 Da ($C_{12}H_{13}O_7^-$) must possess several isomers of similar polarities that absorb in the visible region* (Scheme 1). As a rule, each additional double bond in a conjugated π-electron system is known to shift the absorption maximum about 30 nm towards longer wavelength [24,25]. It follows that conjugation should be less extended in the species that give rise to the $m/z = 289$ anions ($C_{11}H_{13}O_9^-$) (Scheme 2). We have confirmed that $m/z = 289$ anions correspond to C_{11} species because they shift to $m/z = 300.0916$ (versus 289.0565, as detected via high-resolution ESI mass spectrometry) in the photolysis of $^{13}CH_3{}^{13}C(O)^{13}C(O)OH$. The MS/MS spectra of representative $m/z = 247$ and 289 anions reveals systematic 44 (CO_2) and 18 (H_2O) neutral losses, which are characteristic of hydroxyl-acids. Basic chemistry tells us that the various geometric (*E*, *Z*) isomers of the 270 Da acids in Scheme 1 may have different polarities [26] and would absorb further into the visible than the 290 Da acids of Scheme 2 [27,28]. The absorption spectrum of the octa-3,5-diene-2,7-dione motif of most of the proposed structures for the 270 Da acids in fact has maxima at 280 and 350 nm, i.e., it extends significantly into the >400 nm region [29].

It was found that the van Krevelen diagram of the H/C versus O/C ratios of bulk organic aerosols (OA) from a variety of locations and environments has a slope of $S_{VK} \sim -1$ [30]. Since the replacement of a $>CH_2$ group with >C=O and >C—OH functions leads to $S_{VK} = -2$ and 0, respectively, a $S_{VK} \sim -1$ slope is therefore consistent with the creation of both >C=O and >C—OH functionalities, i.e. with the formation of acids or hydroxy-ketones. This has been shown to be true for a wide range of OA types, including laboratory/ambient, biogenic/anthropogenic, urban/remote and freshly emitted/aged. Thus, OA has a characteristic bulk elemental composition with an average $CH_{(2-x)}O_x$ empirical formula [30]. In this context, the empirical formula of colorless $C_{11}H_{14}O_9 \propto CH_{1.27}O_{0.82}$ species shows they are slightly more oxygenated than the expected average: $CH_{1.27}O_{0.73}$, whereas the visible absorbers $C_{12}H_{14}O_7$ (270 Da) $\propto CH_{1.17}O_{0.58}$ are considerably less oxygenated the average species having the same H/C = 1.17 ratio: $CH_{1.17}O_{0.83}$. In other words aerosol 'browness' may not arise from its most oxidized components [11,31]. The basic requirement for bathochromic shifts is the extension of conjugation among preexisting chromophores, in this case C=O carbonyls. The required unsaturations are likely to be created via dehydration of ∝-hydroxy ketones, as we had proposed before [17]. However, they can be partially bleached by photochemically induced rehydration [16,17], and would be destroyed by ozone and OH-radical attack. Thus, 'browness' is not an intrinsic feature of BrC aerosol, but it is expected to vary according to ambient relative humidity, i.e., water activity, and the oxidative power of ambient air, i.e., of insolation.

Notably, $m/z = 177$ signals appear as prominent peaks both at short and long retention times (cf. Figure 3A and C). We had previously identified a C_6-dicarboxylic acid ($C_6H_{10}O_6$, 2,3-dihydroxy-2,3-dimethylsuccinic acid, i.e., dimethyl-tartaric acid, DMT) as a major product of PA photolysis (i.e., at the P1 stage) whose mono-anion gave rise to $m/z = 177$ signals [15]. Since DMT does not absorb above ~250 nm [15], it is likely the species eluting before 10 min. The possibility that the $m/z = 177$ signal appearing

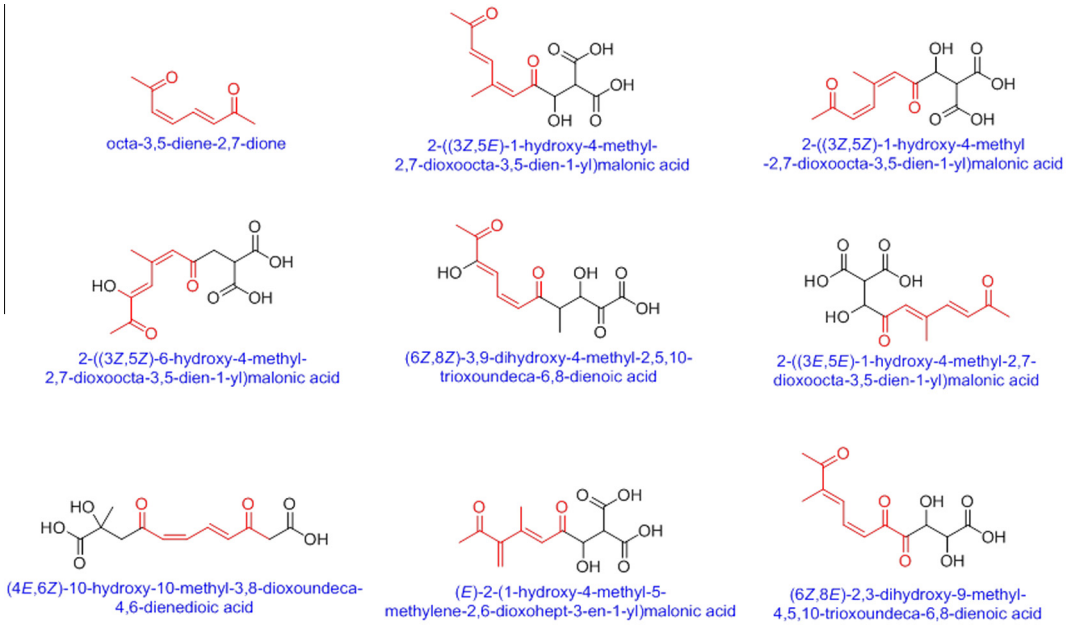

Scheme 1. Proposed structures of the acids giving rise to the ESI mass spectral signals at $m/z = 269$ and the their chromophore.

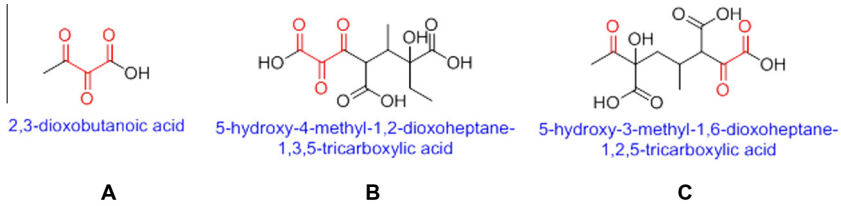

Scheme 2. Proposed structures of the acids giving rise to the ESI mass spectral signals at $m/z = 289$ and their chromophore.

in Figure 3B and C arises from less polar isomers of DMT, such as 2,3,3-trihydroxy-2-methyl-4-oxopentanoic acid, is unlikely because such species can only be gem-diols that would dehydrate into more stable carbonyls. The resulting di-ketones, however, would have given rise to $m/z = 159$ signals, which are conspicuously absent from Figure 3A–C. Thus, we are led to consider that the $m/z = 177$ signal in Figure 3B could be in fact a fragment of higher mass species. The dissimilar retention times of the $m/z = 269$ versus $m/z = 289$ anions could be accounted for by the fact that most conceivable structures of the $m/z = 269$ acids are amphiphilic. Thus, their hydrophobic domains are expected to bind more strongly to the hydrophobic C18-bonded-phase of the reversed-phase column [23].

Summing up, our findings suggest that (1) the visible absorptivity of the aerosol may be due to a small fraction of its chemical components, which is largely comprised of weakly polar species having a significantly smaller O/C ratio than the average, (2) the average oxidation level of the aerosol may not be a good descriptor of its 'brownness'. These conclusions, which are drawn from experiments on basic chemical concepts, should be expected to hold both under laboratory and environmental conditions.

Acknowledgments

This work was supported by NSF (U.S.A.) Grant AC-1238977.

Appendix A. Supplementary data

Supplementary data associated with this article can be found, in the online version, at http://dx.doi.org/10.1016/j.cplett.2014.04.033.

References

[1] N. Unger. Global climate forcing by criteria air pollutants. In: A. Gadgil; D.M. Liverman (Ed.), Annual Review of Environment and Resources, Palo Alto, CA, vol. 37, 2012, pp. 1.
[2] C. Wang, Atmos. Res. 122 (2013) 237.
[3] T.C. Bond et al., J. Geophys. Res.-Atmos. 118 (11) (2013) 5380.
[4] V. Ramanathan et al., Proc. Natl. Acad. Sci. U. S. A. 102 (15) (2005) 5326.
[5] V. Ramanathan, P.J. Crutzen, Atmos. Environ. 37 (2003) 4033.
[6] U.C. Dumka et al., Atmos. Res. 96 (4) (2010) 510.
[7] P. Formenti, W. Elbert, W. Maenhaut, J. Haywood, S. Osborne, M.O. Andreae, J. Geophys. Res.-Atmos. 108 (D13) (2003).
[8] M. Kanakidou et al., Atmos. Chem. Phys. 5 (2005) 1053.
[9] B.J. Williams et al., J. Geophys. Res.-Atmos. 112 (D10) (2007).
[10] T. Nakayama, Y. Matsumi, K. Sato, T. Imamura, A. Yamazaki, A. Uchiyama, J. Geophys. Res.-Atmos. 115 (2010).
[11] A.T. Lambe et al., Environ. Sci. Technol. 47 (12) (2013) 6349.
[12] H.L. Sun, L. Biedermann, T.C. Bond, Geophys. Res. Lett. 34 (17) (2007).
[13] K. Kawamura, E. Tachibana, K. Okuzawa, S.G. Aggarwal, Y. Kanaya, Z.F. Wang, Atmos. Chem. Phys. 13 (16) (2013) 8285.
[14] J.Z. Yu, H.E. Jeffries, K.G. Sexton, Atmos. Environ. 31 (15) (1997) 2261.
[15] M.I. Guzmán, A.J. Colussi, M.R. Hoffmann, J. Phys. Chem. A 110 (2006) 3619.
[16] A.G. Rincon, M.I. Guzman, M.R. Hoffmann, A.J. Colussi, J. Phys. Chem. A 113 (2009) 10512.
[17] A.G. Rincon, M.I. Guzman, M.R. Hoffmann, A.J. Colussi, J. Phys. Chem. Lett. 1 (1) (2010) 368.
[18] K.E. Altieri, S.P. Seitzinger, A.G. Carlton, B.J. Turpin, G.C. Klein, A.G. Marshall, Atmos. Environ. 42 (7) (2008) 1476.
[19] A.G. Carlton, B.J. Turpin, H.J. Lim, K.E. Altieri, S. Seitzinger, Geophys. Res. Lett. 33 (6) (2006).
[20] E. Wiesen, I. Barnes, K.H. Becker, Environ. Sci. Technol. 29 (5) (1995) 1380.
[21] J.H. Seinfeld, S.N. Pandis, Atmospheric Chemistry And Physics: From Air Pollution To Climate Change, second ed., Wiley, Hoboken, N.J., 2006.
[22] J.K. Baker, Anal. Chem. 51 (11) (1979) 1693.
[23] R. Kaliszan, Chem. Rev. 107 (7) (2007) 3212.
[24] A.T. Nielsen, J. Org. Chem. 22 (12) (1957) 1539.
[25] D.L. Pavia, Introduction To Spectroscopy, 4th ed., Brooks/Cole, Belmont, CA, 2009.
[26] E.V. Anslyn, D.A. Dougherty, Modern Physical Organic Chemistry, University Science Books, Sausalito, California, 2006.
[27] S. Francese, R. Bradshaw, B. Flinders, C. Mitchell, S. Bleay, L. Cicero, M.R. Clench, Anal. Chem. 85 (10) (2013) 5240.
[28] R.M. Silverstein, F.X. Webster, D.J. Kiemle, Spectrometric Identification Of Organic Compounds, seventh ed., John Wiley & Sons, Hoboken, NJ, 2005.
[29] P. Karrer, C.H. Eugster, S. Perl, Helv. Chim. Acta 32 (3) (1949) 1013.
[30] C.L. Heald et al., Geophys. Res. Lett. 37 (2010).
[31] C.D. Cappa, D.L. Che, S.H. Kessler, J.H. Kroll, K.R. Wilson, J. Geophys. Res.-Atmos. 116 (2011).